Wireless Multimodal Neural Interface Device for Neural Control Studies

[1]Linran Zhao, [2]Yan Gong, [2]Wen Li, and [1]Yaoyao Jia
[1]Department of Electrical and Computer Engineering, The University of Texas at Austin, Austin, TX, U.S.A
[2]Department of Electrical and Computer Engineering, Michigan State University, East Lansing, MI, U.S.A

***Abstract*—We present a wireless multimodal neural interface device to record neural activities of neurons in dorsal root ganglia (DRG) and muscle electrical activities (EMG) of the selected muscles of 4 limbs, while selectively manipulating neural activities in DRGs of freely locomoting cats via optogenetic stimulation. The neural interface device has 4 identical 8-channel analog front-end (AFE) circuits for DRG recording with the mid-band gain of 60 dB within 9 Hz – 500 Hz, as well as a 16-channel AFE for EMG recording with the mid-band gain of 40 dB within 0.7 Hz – 105 Hz. To effectively stimulate target neurons by optogenetic neuromodulation, the neural interface device has 4 identical 4-channel programmable stimulation drivers that can deliver pulsating current up to 65 mA to the selected LED. To eliminate tethering effects, the neural interface device uses Bluetooth Low Energy radio to receive user-defined stimulation parameters (i.e., stimulation frequency, pulse width, LED current) and send the recording data. The neural interface is built in a form factor of a head-mounted device, or headstage device, which has a plug-in structure formed by two vertical functional boards and one horizontal substrate board, resulting in dimensions of 3 × 3 × 3.3 cm^3 and a weight of 6.5 g.**

Keywords—neural recording, dorsal root ganglia, muscle electrical activities, optogenetic stimulation, analog front-end, programmable stimulation, wireless, multifunctional

I. Introduction

When animals move, the receptors in moving limbs inform the central nervous system (CNS) with somatosensory feedback from muscle spindle afferents [1]. The CNS integrates the feedback information at various levels and shapes locomotor output to adapt locomotion to the constantly changing environment [1]. Thus, motion-dependent somatosensory feedback is critical in the control of functional and dynamically stable locomotion. Neural interface devices, providing accurate modification and measurement of target analytes in animals and humans, have always been important in investigating the mechanisms of somatosensory feedback in the control of locomotion [2]-[4]. Over the past years, there have been exciting advancements in the development of neural interface devices, involving the development of new flexible sensing materials, low power and high-density circuits, wireless telemetry, integrated implantable and wearable form factors, etc.

Neural interface devices capable of injecting a designated amount of charge into the target neural tissues to modulate neural activities have been proven effective to partially restore tactile perception by electrical stimulation of the residual cutaneous nerves [2]-[4]. However, electrical stimulation suffers from indiscriminate stimulation of spindle afferents and poor spatial resolution due to unpredictable current pathways [5].

This work is supported in part by the NSF award ECCS-2024486 and NSF ASSIST Center ERC (EEC-1160483).

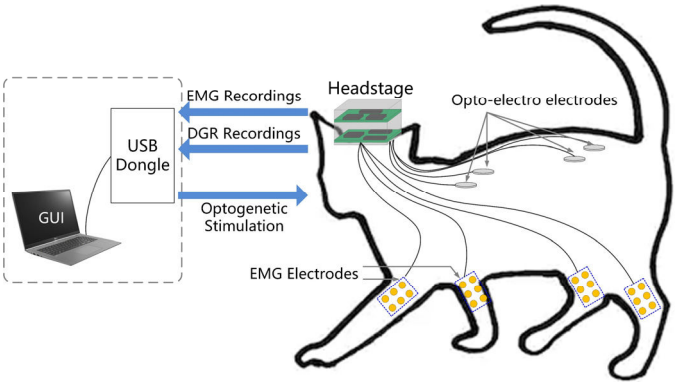

Fig. 1. Conceptual view of the system setup for operating the wireless multimodal neural interface device on freely locomoting cat.

Emerging optogenetic stimulation with distinct advantages over electrical stimulation, such as cell-type specificity, sub-millisecond temporal precision, and rapid reversibility can potentially substitute/complement traditional neuromodulation [5, 6]. Thus, neuroscientists have proposed strategies to selectively manipulate spindle afferent activities in animal subjects via optogenetic stimulation of the target neurons in dorsal root ganglion (DRG) [7, 8]. In addition to optogenetic stimulation of target DRG neurons, another indispensable step for a better understanding of somatosensory locomotion control is to record neural activities of target DRG neurons and measure muscle electrical activities (EMG) [1]. The recording data can be used as feedback mechanisms for researchers to optimize stimulation parameters in terms of stimulation efficacy, safety, and power efficiency in what is known as closed-loop neuromodulation [9, 10].

Despite advances in the design of stimulation and recording circuitry, neural interface device also requires an efficient electronic communication interface for reliable wireless operation. Current choices of neural interface devices for optogenetic stimulation are limited to lasers or LEDs [5]. Lasers and laser diodes use narrow spectral bandwidth to produce high light intensity with low beam divergence [5]. However, they require high power consumption, slow warm-up time, and the use of tethered optic fibers to steer the light. The tethered optical fibers impose several limitations for studies on freely locomoting animals, including potentially biased behavior outcomes, cable tangling or breakage during experiments, and potential discomfort/stress of the animal subjects [11]. On the other hand, LEDs offer many advantages over their laser counterparts, including low cost, power efficiency, stable illumination, compact size, fast response, and compatibility with wireless telemetries [5, 12].

2021 IEEE Biomedical Circuits and Systems Conference (BioCAS) | 978-1-7281-7204-0/21/$31.00 ©2021 IEEE | DOI: 10.1109/BIOCAS49922.2021.9644933

978-1-7281-7204-0/21/$31.00 ©2021 IEEE

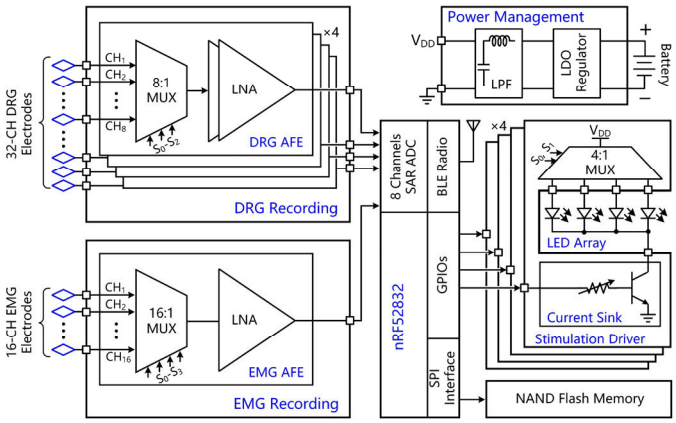

Fig. 2. Block diagram of the headstage circuitry.

To address the above-mentioned requirements, we develop a wireless multimodal neural interface device. The neural interface device, designed in the form of a headstage and tailored for freely locomoting cats, is capable of optogenetic stimulation, DRG neural recording, EMG recording, sensory data saving, and wireless data communication with a data aggregator (i.e., a USE dongle).

II. System Overview

Fig. 1 shows the conceptual view of the experimental setup, including the headstage and wireless telemetry, for performing neural control studies on freely locomoting cats. There is a Bluetooth Low Energy (BLE) link between the headstage and the USB dongle. A graphical user interface (GUI) running on a PC performs parameter setting, data representation, processing, and storage. The headstage wirelessly receives stimulation parameters set by the user in the GUI to selectively drive the LEDs while sending the amplified, filtered, and digitalized recording data to the USB dongle via the BLE link. Four flexible opto-electro microelectrode arrays are implanted bilaterally in DRGs of spinal segments of L5, L7, C6, and C7. Each implant is built on a flexible parylene film that carries 4 addressable LEDs and 8 epidural recording microelectrodes. The headstage connects to the 4 implants through 4 clusters of insulated wires that are placed under the skins running along the spinal cord. The headstage enables one implant at a time to perform optogenetic stimulation and neural recording of target neurons in one DRG. Besides, the headstage read EMG signals from a cluster of 16 insulated wires that are placed under the skin and run down to the selected muscles of the 4 limbs of the freely locomoting cat.

The simplified block diagram of the headstage circuitry is shown in Fig. 2. The battery output is stabilized by an adjustable regulator (ADP165) and further low-passed filtered (LPF) to generate a supply voltage, V_{DD} = 3.3 V. The headstage has 4 identical stimulation drivers, each of which employs a 4:1 multiplexer (MUX) and a current sink formed by a bipolar junction transistor (BJT) and a digital potentiometer (POT) (AD5242) to control the 4 LEDs assembled on the DRG implant. Specifically, once the nRF52832 microcontroller unit (MCU) receives stimulation parameters (e.g., frequency, pulse width, and current), the general-purpose I/O (GPIO) ports generate stimulation pulses based on the user-defined pattern to drive the BJT through the digital POT and set the 4:1 MUX to switch on the selected LED. The stimulation current flowing through the selected LED is adjustable by adjusting the resistance of the digital POT.

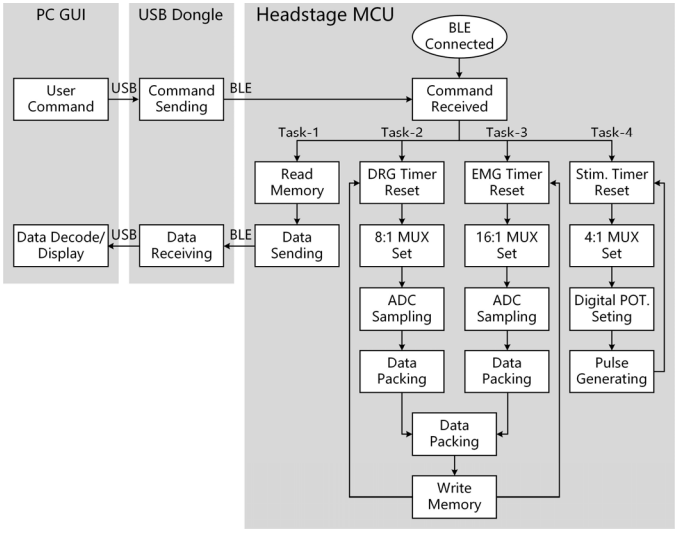

Fig. 3. Simplified flowchart of the data control algorithm in the system.

The DRG recording circuitry includes 4 identical AFE channels. Each AFE, in which two low-noise amplifiers (LNA) in series amplify and filter the input signals via time-division multiplexing, performs 8-channel DRG recording. The headstage also includes a single channel AFE with time-division multiplexing of input signals for 16-channel EMG recording. The LNA design using amplifiers (MCP6141) for both DRG and EMG recording can refer to the design in our previous work [13]. Stimulus artifacts are rejected by disconnecting the AFEs from electrodes during stimulation pulses to enable recording shortly after stimulation. The built-in analog-to-digital converter (ADC) of the MCU digitizes the DRG and EMG AFE outputs. To reduce the data loss, the MCU packetizes the digitized data and writes data in a NAND flash memory (MT29F1G) before sending the recording data to the USB dongle via BLE link.

The headstage MCU mainly performs 4 independent tasks, as shown in Fig. 3. Once the BLE connection is established, user commands are delivered to the USB dongle and sent on the fly to the MCU. In Task-2, once the DRG recording function is enabled, the MCU activates one DRG AFE by setting the 8:1 MUXs. The built-in ADC captures data samples from each channel of the selected DRG AFE at a sampling rate of 10 kHz. If Task-3 is enabled at the same time, to synchronize the EMG recording with the DRG recording, the build-in ADC takes one EMG sample for every 8 data samples taken from one DRG AFE, resulting in the 625 Hz sampling rate of each EMG channel. After taking one data sample from all 16 EMG channels, the MCU packetizes the 16 EMG samples with 128 DRG samples into one package and writes the package in the memory. Once Task-4 is launched, the MCU sets the 4:1 MUXs to select the target LED while configuring the digital POT. Based on user-defined parameters, the MCU GPIOs output stimulation pulses. To synchronize stimulation with DRG recording for offline data analysis, the two functions will use the same timer. When Task-1 is triggered, the MCU reads the saved recording data from the memory while wirelessly transmitting the data to the USB dongle via BLE.

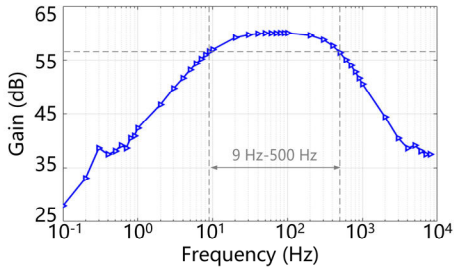

(a)

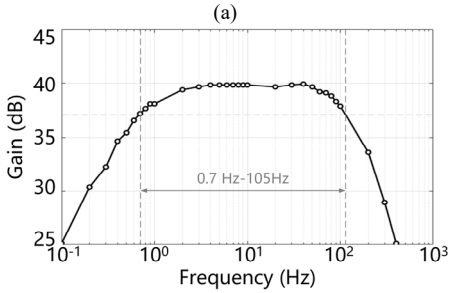

(b)

Fig. 4. Measured frequency response of (a) the DRG AFE and (b) the EMG AFE.

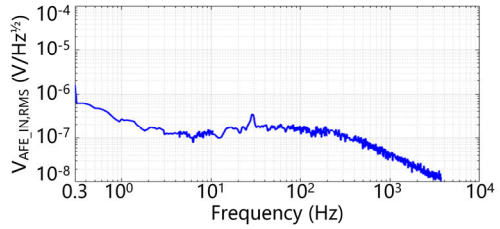

(a)

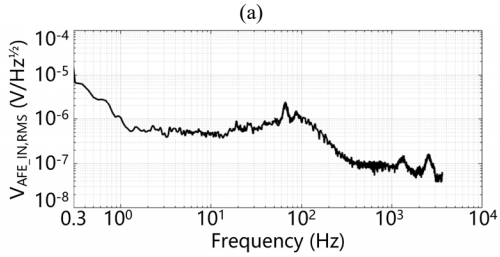

(b)

Fig. 5. Measured input-referred noise spectrum of (a) the DRG AFE and (b) the EMG AFE.

III. Measurement Results

Fig. 4 shows the measured frequency response of the DRG and EMG AFE channels. The mid-band gain of the DRG AFE is relatively constant at 60 dB within the 9 Hz to 500 Hz band of interest. The EMG AFE has a relatively constant gain of 40 dB within the frequency band of 0.7 Hz-105 Hz. Fig. 5a presents the measured DRG AFE input-referred noise spectrum. The 1/f noise corner occurs at 6 Hz. Integration under the curve from 9 Hz to 500 Hz yields a root mean square (RMS) noise voltage of 3.35 μV_{RMS} for the DRG AFE. In Fig. 5b, the 1/f noise corner frequency is at 1.2 Hz due to the relatively high thermal noise level. The RMS noise voltage of the EMG AFE is 5.02 μV_{RMS} by integrating the curve from 0.7 Hz to 105 Hz.

Fig. 6a presents the measurement results of current pulses delivered to the selected LED (220×270×50 μm^3, TR2227TM, Cree) with 10 ms pulse width at a rate of 1.25 Hz when the

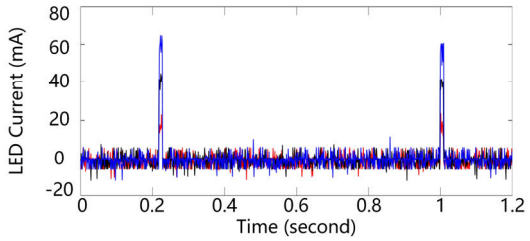

(a)

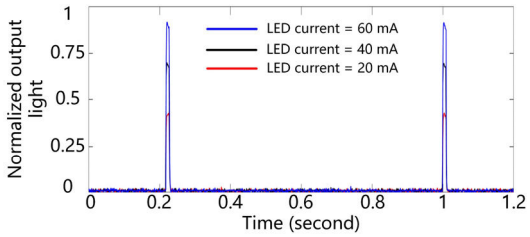

(b)

Fig. 6. Measured transient waveforms of (a) LED current at 3 stimulation current settings and (b) normalized LED output light at 3 LED current values.

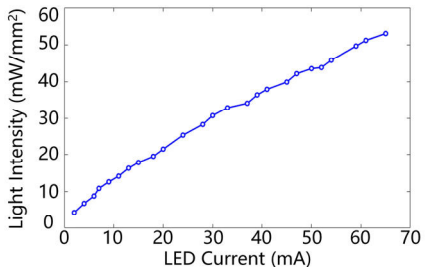

Fig. 7. Measured light intensity of the selected LED as a function of the LED current.

headstage operates optogenetic stimulation. The LED current is measured from the voltage across a 10 Ω current-sensing resistor in series with the LED. The LED current increases from 20 mA to 60 mA according to the stimulation current settings. The LED output light during stimulation pulses is also measured at each current level, as shown in Fig. 6b. The emitted light from the selected LED is collected by a photodetector (Newport 818-SL) connected to an optical power meter (Newport 2936-R). The normalized output light expectedly followed the stimulation current variation with a slight delay.

Fig. 7 shows the light intensity under different current settings, which matches the LED specifications. At the minimum current of 2 mA, the light intensity is 4.3 mW/mm^2, which is above the 1 mW/mm^2 threshold of effective optogenetic neuromodulation [14]. The LED current increasing to 65 mA yields a light intensity of 53.2 mW/mm^2. Measured specifications of the headstage are summarized in Table I.

The *in vitro* experiment is a major step towards conducting *in vivo* experiments on freely locomoting cats using the same system. Fig. 8a shows the *in vitro* setup using tissue layer for preliminary evaluation of the wireless neural recording operation. The headstage, powered by a 550 mAh rechargeable LiPo battery, is placed on a piece of beef. The headstage consists of three PCBs, two of which are mounted vertically on a base board. The two vertically-mounted PCBs hold all commercial off-the-shelf (COTS) components and are detachable from the base board. The base board provides contacts with the 4 opto-

TABLE I: MEASURED HEADSTAGE SPECIFICATIONS

Overall Device		
Headstage size		3 × 3 × 3.3 cm^3
Headstage weight		6.5 gram
Power consumption (with all functions on)		28.5 mW
Power consumption (with BLE connected)		1.8 mW
AFE	**DRG Recording**	**EMG Recording**
# of channels	32	16
Mid-band gain	60 dB	40 dB
Bandwidth	9 Hz – 500 Hz	0.7 Hz – 105 Hz
Input-referred noise	3.35 μV_{RMS}	5.02 μV_{RMS}
Optogenetic Stimulation		
Frequency		1 Hz – 500 Hz
Pulse width		1% – 50% duty cycle
Current limiter		2 mA – 65 mA
Light intensity		4.3 – 53.2 mW/mm^2
Date Transmission		
DRG sampling rate		10 kHz per channel
EMG sampling rate		625 Hz per channel
ADC ENOB		8 bits
Data package		144 bytes
Transmission range		1-5 meters

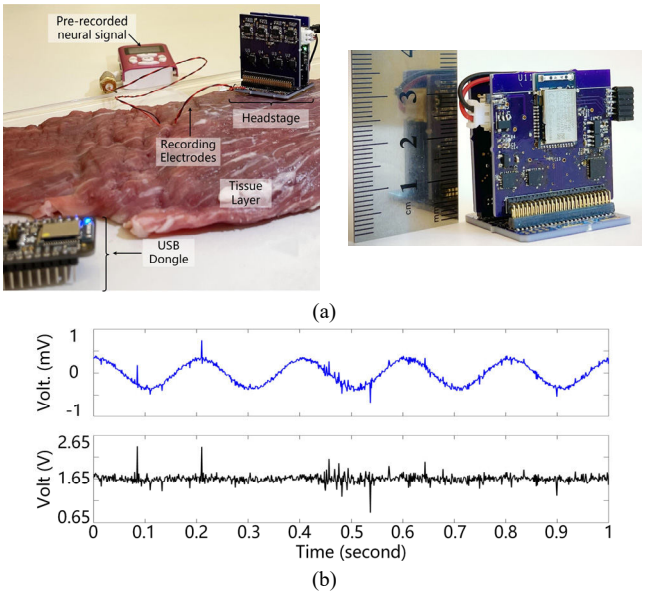

Fig. 8. (a) *In vitro* measurement setup with a close-up view of the headstage. (b) Recovered recording data from the pre-recorded neural signal.

electro microelectrode arrays and will be encapsulated with Parylene-C and PDMS before being attached to animal subject's head for *in vivo* studies. The battery is sandwiched between the two vertically-placed PCBs. The headstage with dimensions of 3×3×3.3 cm^3 and weight of 6.5 g will not cause discomfort or interference with free locomotions of the animal subject.

To emulate a real recording, a pre-recorded neural signal, containing spikes in hundreds of μV_{PP} ranges plus a 5 Hz sinewave, is applied to the tissue. The DRG AFE is set to filter out the 5 Hz sinewave and extract the spikes. Recording data is wirelessly transmitted via the BLE to the USB dongle for data recovery. Fig. 8b shows a short 1-second interval of the pre-recorded neural signal that is applied to the DRG AFE channel (upper trace) and the recovered data on the Rx side (lower trace). The spikes are separated from the 5 Hz sinewave by high-pass filtering and can be recovered with high fidelity, which demonstrates the functionality of the device *in vitro*.

IV. CONCLUSION

We have presented a wireless multimodal neural interface device for DRG recording, EMG recording, and optogenetic stimulation. The DRG and EMG AFE circuits offer low-noise signal sensing performance. Saving recording data in the NAND flash memory can significantly reduce the risk of data loss. The stimulation driver can deliver large instantaneous current pulses up to 65 mA to the selected LED, allowing the light flashes produced to surpass the optogenetic neuromodulation threshold. The BLE link between the headstage and the USB dongle allows for wireless operation of these neural interfacing functions, achieving an untethered system. The functionality of the headstage device has been evaluated in benchtop and *in vitro* settings. In our next step, we will use the same device and supporting necessary components to conduct neural recording and stimulation experiments on freely locomoting cats.

REFERENCES

[1] D. H. Edwards, B. I. Prilutsky, Sensory feedback in the control of posture and locomotion, Neurobiology of Motor Control: Fundamental Concepts and New Directions, Hoboken Wiley, NJ, pp. 263–304, Sept. 2017.

[2] A. Shon, K. Brakel, M. Hook, and H. Park, "Fully implantable plantar cutaneous augmentation system for rats using closed-loop electrical nerve stimulation," *IEEE Trans. Biomed. Circuits Syst.*, vol. 15, no. 2, pp. 326-338, Apr. 2021.

[3] I. Williams, E. Brunton, A. Rapeaux, Y. Liu , S. Luan, K. Nazarpour, and T. G. Constandinou, "SenseBack-an implantable system for bidirectional neural interfacing," *IEEE Trans. Biomed. Circuits Syst.*, vol. 14, no. 5, pp. 1079-1087, Oct. 2020.

[4] M. Heravi, K. Maghooli, F. N. Rahatabad, R. Rezaee, "Application of a neural interface for restoration of leg movements: intra-spinal stimulation using the brain electrical activity in spinally injured rabbits," *J. Appl. Beimed*., vol. 18, no. 2-3, pp. 33-40, Jan. 2020.

[5] B. Fan and W. Li, "Miniaturized optogenetic neural implants: a review," *Lab on a Chip*, vol. 15, no. 19, pp. 3833-3855, Aug. 2015.

[6] S. Goncalves, J. Ribeiro, A. Silva, R. Costa, and J. Correia, "Design and manufacturing challenges of optogenetic neural interfaces: a review," *J. Neural Eng.,* vol. 14, no. 4, p. 041001, May 2017.

[7] A. Santuz, T. Akay, W. P. Mayer, T. L. Wells, A. Schroll, A. Arampatzis, "Modular organization of murine locomotor pattern in the presence and absence of sensory feedback from muscle spindles." *J. Physiol.*, vol. 597, no. 12, pp. 3147-3165, Mar. 2019.

[8] O. D. Laflamme and T. Akay, "Excitatory and inhibitory crossed reflex pathways in mice," *J. Neurophysiol*., vol. 120, no. 6, pp. 2897-2907, Nov. 2018.

[9] R. Sitaram, T. Ros, L. Stoeckel, *et al.*, "Closed-loop brain training: the science of neurofeedback," *Nat. Rev. Neurosci.,* vol. 18, no. 2, pp. 86-100, Feb. 2017.

[10] T. Levi, P. Bonifazi, P. Massobrio, and M. Chiappalone, "Closed-loop systems for next-generation neuroprostheses," *Front. Neurosci.,* vol. 12, p. 26, Feb. 2018.

[11] Y. Jia, S. A. Mirbozorgi, Z. Wang, C-C Hsu, T. E. Madsen, D. Rainnie, M. Ghovanloo, "Position and orientation insensitive wireless power transmission for EnerCage-Homecage system," *IEEE Trans. Biomed. Circuits Syst.*, vol. 64, no. 10, pp. 2439-2449, Apr. 2017.

[12] K. Y. Kwon, H.-M. Lee, M. Ghovanloo, A. Weber, and W. Li, "Design, fabrication, and packaging of an integrated, wirelessly-powered optrode array for optogenetics application," *Front. Syst. Neurosci.*, vol. 9, p. 69, May 2015.

[13] Y. Jia, U. Guler, Y.-P. Lai, Y. Gong, A. Weber, W. Li, and M. Ghovanloo "A trimodal wireless implantable neural interface system-on-chip," *IEEE Trans. Biomed. Circuits Syst.*, vol. 14, no. 6, pp. 1207-1217, Dec. 2020.

[14] E. Stark, T. Koos, and G. Buzsaki, "Diode probes for spatiotemporal optical control of multiple neurons in freely moving animals," *J. Neurophysiol.*, vol. 108, no. 2, pp. 349-363, Jul. 2012.